

# Influence of TiN/Ti Coating on the Erosion Resistance against Solid Particles

Yan Chai\*; Guangyu He; Yuqin Li; Zhufang Yang

Science and Technology on Plasma Dynamics Laboratory, Air Force Engineering University, Xi'an 710038, China

\*chaiyan1026@163.com

## Abstract

Aero-engine usually adopts titanium alloys as the compressor blade materials. Owing to their low hardness, however, the solid particle erosion (SPE) resistance of titanium alloys is also very low, and the TiN/Ti coating is an effective method to improve the anti-erosion performance of titanium alloys. To design the structure of TiN/Ti coating and acquire coatings with good performance, the equivalent plastic strain distribution of single layer, three layers, six layers and twelve layers of TiN/Ti coating after erosion by single sand is calculated and the results show that if the total thickness of the coating is constant (3 $\mu$ m), the more the layers are, the better the coating's anti-erosion performance will be. In other ways, the coating erosion-resistant experiments also prove that the SPE resistance of multi-layer coating is excellent.

## Keywords

Titanium Alloys; Erosion; TiN/Ti Coating; Structure

## Introduction

Titanium alloys are commonly used in compressor blade of Aero-engines to obtain a higher thrust-weight ratio[1]. But, because of their low hardness and poor wear resistance, and under the impact of high-speed dust, sand and other solid particles, the compressor blade shape and structural integrity will inevitably be damaged (shown in Fig.1), significantly reducing the aero-engine's performance and service life[2].



FIGURE 1. AERO-ENGINE COMPRESSOR BLADE EROSION

Hard coating is an effective method to improve aero-engine blade's resistance against sand and dust erosion[3-5]. The multi-layer ceramic-metallic coating is attracting much attention due to its high surface hardness, excellent tenacity, and the diverse structure and surficial morphology[6-8]. But under some rushed corrosion conditions, the anti-corrosion performance of multi-layer coating is significantly declined compared with the single-layer coating[9-11]. Furthermore, for the same thickness of multi-layer ceramic-metal coating, the erosion resistance is significantly affected by the thickness of the middle ductile layer, the proportion of ceramic to metallic coatings, and also the number of coating layers. The multi-layer TiN/Ti coating structural design and the study on the solid particle erosion resistance of TC4 alloy are conducted in this paper.

## Experimental Procedure

TC4 titanium alloy was used in this experiment. Its main chemical components are shown in Table.1 and the specimen size of 50mm  $\times$  20mm  $\times$  4mm was used with No1500 sandpaper for polish processing.

The preparation of the coating specimens were completed in the Northwest Research Institute of Nonferrous Metals using magnetron sputting equipment, cleaned by 0.02Pa argon gas and the washing bias voltage was -

700V~1000V. The magnetron sputtering deposition equipment was used to prepare coating in the cleaned specimens. The process control parameters are as follows: substrate bias voltage -400V, titanium target current 60~100A, aluminum target current 60A, nitrogen pressure 0.2 Pa. On the substrate, the first layer coating is titanium and the second layer coating is TiN. After multi-crossing deposition, a multi-layer TiN/Ti coating was eventually prepared. The repeating structural unit in the sedimentary thickness is called  $\lambda$ , and the thickness ratio of modulation layer A(Ti), i.e.,  $I_A$  to that of layer B(TiN), i.e.,  $I_B$  during one modulation cycle is called modulation ratio. This modulation ratio is 1:3, and the modulation cycle is 500nm. The structure and macroscopic image of multi-layer TiN/Ti coating are shown in Fig.2, respectively.

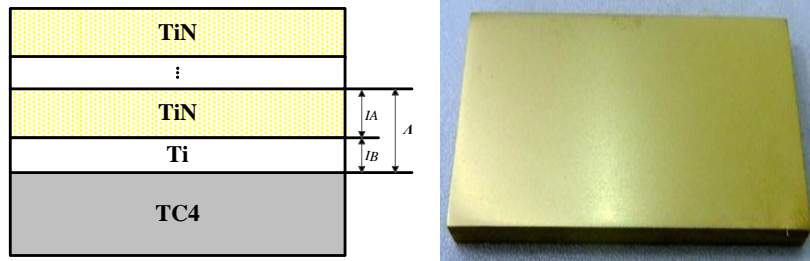


FIGURE 2. MULTILAYER TIN/TI COATING STRUCTURE AND MACROSCOPIC IMAGE

The JEOL/JSM-6360LV Scanning electron microscopy ( SEM ) was employed to observe the cross section of the specimens shown in Fig.2, and the microstructure of the TiN/Ti coating is shown in Fig. 3. From Fig.3, it can be seen that the coating thickness is approximately 7  $\mu\text{m}$ , and the coating layers of different modulation cycles are clearly uniform in their thickness.

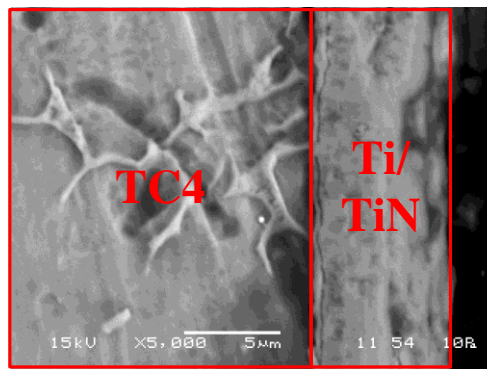


FIGURE 3. MULTI-LAYERS TIN/TI COATING CROSS SECTION SEM MORPHOLOGY

In this paper, the simulation research was mainly carried out on fine sand (size  $d < 100 \mu\text{m}$ ). The whole process of sand impacting to the blade surface coating and the changes in stress and strain as well as the stress concentration were calculated. In the analysis, in order to facilitate modeling, the blade was assumed stationary, and the sand grains were crashing onto the blade surface with high speed.

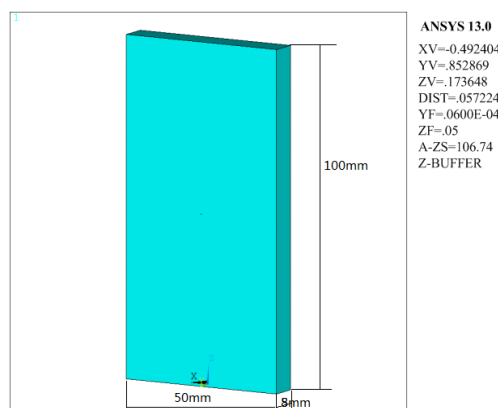


FIGURE 4. FLAT-BLADE MODEL OF TC4 ALLOY (50MM×8MM×100MM)

In calculation, the flat-blade model was adopted (Fig.4). The blade thickness was selected as 8mm, width as 50mm and highness as 100 mm. Spherical Al<sub>2</sub>O<sub>3</sub> dust with a diameter of 50 μm was employed to impact the single-layer, three-layer, six-layer and twelve-layer coatings at 84 m/s. After impacting, the coating protection performance with different structures was measured by the equivalent plastic strain of the substrates. If the equivalent plastic strain is small, then the protection is good. Taking into account that the coating thickness does not influence the dimensional accuracy of the protected parts, the thickness in numerical simulations was assumed unchanged (3 μm). The substrate material is titanium alloy, the hard coating layer is TiN, and the transition layer is titanium.

**Results And Discussion**

Using above parameters to calculate, the coating structure and the equivalent plastic strain distribution after erosion are shown in Fig.5~ Fig.8.

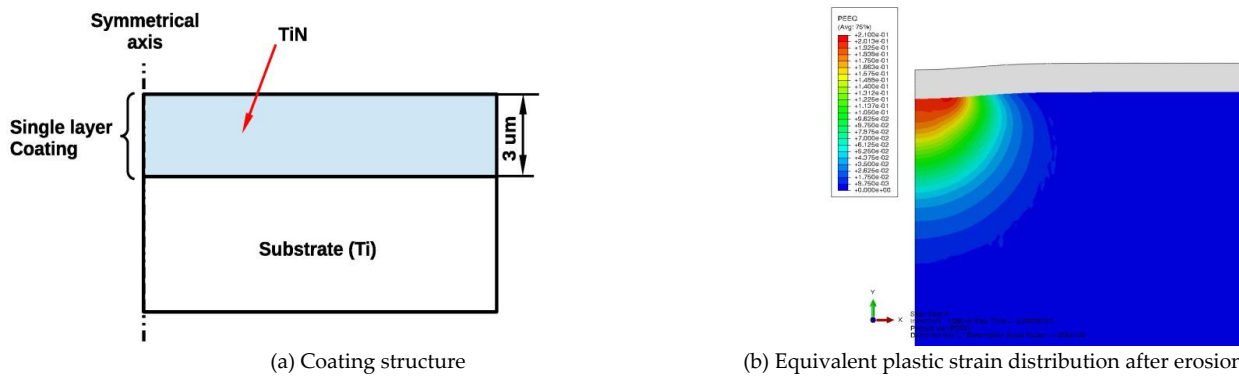


FIGURE 5. EQUIVALENT PLASTIC STRAIN DISTRIBUTION OF SINGLE-LAYER COATING AFTER EROSION BY SINGLE SAND

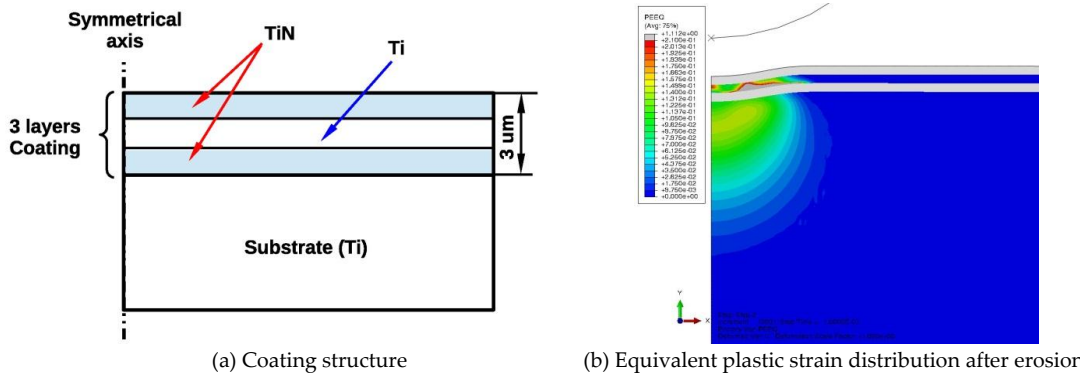


FIGURE 6. EQUIVALENT PLASTIC STRAIN DISTRIBUTION OF THREE-LAYER COATING AFTER EROSION BY SINGLE SAND

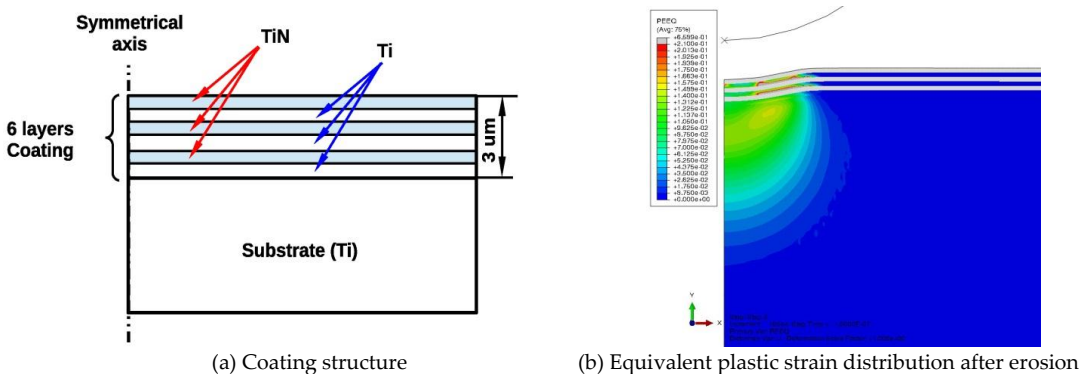


FIGURE 7. EQUIVALENT PLASTIC STRAIN DISTRIBUTION OF SIX-LAYER COATING AFTER EROSION BY SINGLE SAND

From Fig.5, it can be seen that the equivalent plastic strain distribution at the sample interface between substrate and coating is largest, reaches a value of 0.21.

From Fig.6, it can be seen that after erosion on three-layer coating, the equivalent plastic strain in transition layer

(Ti) is the largest and the value is 0.21, and that at the interface between substrate and coating is 0.13.

From Fig.7, it can be seen that after erosion by single sand, the equivalent plastic strain in transition layer (Ti) is the largest and the value is 0.20, and that at the interface between substrate and coating is 0.12.

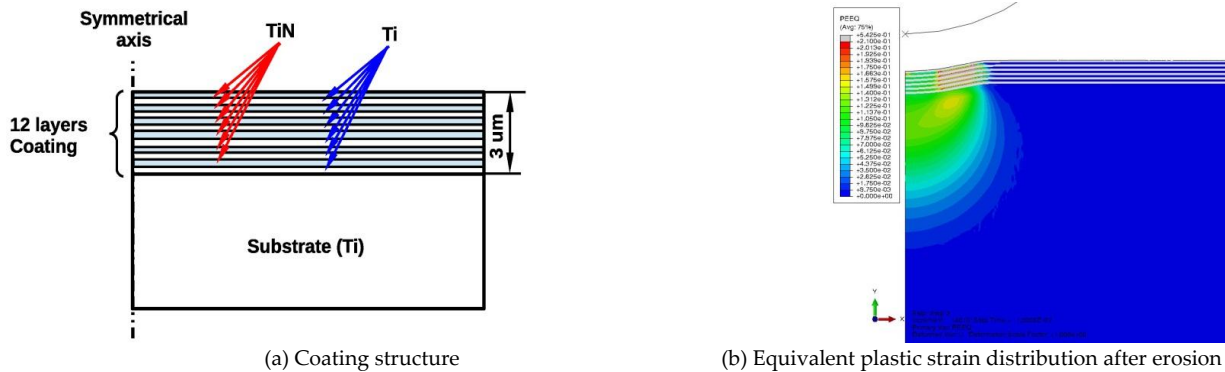


FIGURE 8. EQUIVALENT PLASTIC STRAIN DISTRIBUTION OF TWELVE-LAYER COATING AFTER EROSION BY SINGLE SAND

From Fig.8, it can be seen that after erosion on twelve-layer coating by single sand, the equivalent plastic strain in transition layer (Ti) is the largest, reaching 0.19, and the equivalent plastic strain at the interface between substrate and coating is 0.11.

The largest equivalent plastic strain distribution of different coating structures is summarized in table 2.

From Fig.5~Fig.8 and table 2, it can be seen that when the coating structure is single-layer and eroded by single sand, the substrate material produces large plastic deformation and the protection of coating is not good. If the coating structure is multi-layer, the substrate material produces smaller plastic deformation than single-layer coating. The more the plastic deformation produced by the material is, the more it is prone to failure. The plastic deformation of the multi-layer coating is smaller than that of the single-layer coating structure. Therefore, it is not easy to fail, which means that the protective effect of the multi-layer coating is better than that of the single-layer coating.

In addition, the transition layer of the multi-layer coating produced a plastic deformation larger than the substrate material, and the plastic deformation decreases with the increase of coating layers. This indicates that coating bears most of the plastic deformation caused by sand dust erosion, and thus plays a role in the protection of the substrate. The more the coating layers are, the smaller the plastic deformation in each layer is, and the more difficultly the substrate is prone to failure, so the multi-layer coating has better protection effect on the substrate.

**Tables**

TABLE 1 TC4 CHEMICAL COMPOSITION OF TITANIUM ALLOYS (WT%)

Composition	Al	V	Fe	C	N	H	O	Ti
Percent (wt%)	6.06	3.92	0.3	0.013	0.014	0.0014	0.15	Bal

TABLE 2 THE LARGEST EQUIVALENT PLASTIC STRAIN DISTRIBUTION AND THE EQUIVALENT PLASTIC STRAIN DISTRIBUTION BETWEEN SUBSTRATE AND COATING WITH DIFFERENT STRUCTURES AFTER SINGLE-SAND EROSION

coating structure	the largest equivalent plastic strain distribution	the largest equivalent plastic strain	the equivalent plastic strain between substrate and coating
Single-layer	interface between substrate and coating	0.21	0.21
Three-layer	transition layer	0.21	0.13
Six-layer	transition layer	0.20	0.12
Twelve-layers	transition layer	0.19	0.11

**Conclusions**

The simulation results show that after the single-layer coating is eroded by sand, there is a plastic deformation in

the substrate, and the maximum plastic deformation is located on the surface of the substrate, so the substrate produces failure earlier than the coating, which means that the protective effect of the coating is not obvious. After the multi-layer coating is eroded, the plastic deformation of the substrate is smaller than that of single-layer coating, so the substrate is more difficult to be protected by the multi-layer coating than single-layer coating. In addition, the maximum plastic deformation of specimen with multi-layer coating take places in transition layer, and the maximum plastic deformation is not only lower than that of the single-layer coating, but decreases with the increase of the coating layers as well. Therefore, after the specimen protected by multi-layer coating is eroded by single sand, the failure occurs first in the coating, thereby protecting the substrate material from sand erosion. Thus, the multi-layer coating has better protection effect on the substrate.

#### ACKNOWLEDGEMENTS

This research paper is supported by the National Natural Science Foundation of China(51405506) and in the research process, the Northwestern Polytechnical University and the Northwest Research Institute of Nonferrous Metals offer us a lot of help and we really appreciate them.

#### REFERENCES

- [1] Jin Hexi, Wei Kexiang and Li Jianming: 'Research development of titanium alloy in aerospace industry', *The Chinese Journal of Nonferrous Metals*, 2015, 22(2),280–292.
- [2] Zhao Dandan: 'Development and application of Titanium alloys in the aviation', *Foundry*, 2014,63(11), 1114–1117.
- [3] Fu Li, Chen Xiaoming and Zhao Jian: 'Study on microstructure and wear properties of WC/Co coating', 2014, 43(20),103–105.
- [4] Wang Aiqing, Liu Pei and Xie Jingpei: ' Erosion wear behavior of low chromium cast iron containing nickel', 2014, 26(8), 37–41.
- [5] Zhou GH, DING HY and Zhang Y: 'Corrosion-erosion wear behaviors of 13Cr24Mn0.44N stainless steel in saline-sand slurry', *Tribology International*,2010,43,paper891.
- [6] Liu Hongwei, Zhu Sheng and Yin Fengliang: ' Progress on TiB<sub>2</sub>-TiC/Ti(C,N) composite coatings', 2013, 27(7),42–45.
- [7] M.Bromark, M.Larsson, P.Hevenqvist and S.Hogmark: 'Wear of PVD Ti/TiN multi-layer coatings, *Surface and Coatings Technology*', 1997, 90(3) ,217–223.
- [8] L.A. Dobrzanski and K. Lukaszkowicz: 'Erosion resistance and tribological properties of coatings deposited by reactive magnetron sputtering method onto the brass substrate', *Journal of Materials Processing Technology*, 2004,157–158,317–323.
- [9] A.Leyland and A.Matthews: 'Thick Ti/TiN multilayered coatings for abrasive and erosive wear resistance, *Surface and Coatings Technology*', 1994,70 ,19–25.
- [10] Zhao Jianhua, Zhao Zhanxi and Chen Xiaoliang: ' Microstructure and anti-erosion wear properties of CrMoV alloying coating',2015, 34(10), 111–114.
- [11] He Guangyu, Li Yinghong and Wang Jian: ' Anti-erosion coating technique based on plasma and its application in helicopter aero-engines', 2014, 40(7),2133–2139.

# Strength Enhancement of Stereolithography Parts

Raju B S<sup>1</sup>, Chandra Sekhar U<sup>2</sup>, Drakshayani D N<sup>3</sup>

<sup>1</sup>Associate Professor, School of Mechanical Engineering, Rukmini Knowledge park, REVA university, Bangalore:560064, Karnataka, India.

<sup>2</sup>Former Scientist G, GTRE & Director, Institution of Engineers (India), Gachibowli, Hyderabad-32, India

<sup>3</sup>Professor, Department of Mechanical Engineering, Sir.M.VIT, Bangalore, Karnataka, India

rajubsgowda@gmail.com, rapidchandra@gmail.com, dndrakshayani@gmail.com

## Abstract

The paper presents the detailed experimental investigation on built parameters of the prototypes by Stereolithography process which uses SL5530 epoxy resin material. Test specimens were fabricated on a SLA 5000 machine manufactured by 3D systems and experiments were carried out for an optimal parametric combination in order to obtain favorable quality characteristic using the Taguchi based Grey relational analysis. A plan of experiments, based on the technique of Taguchi, was performed. Analysis of Variance was used to investigate the quality characteristics of Stereolithography parts. The objective was to establish a correlation between the layer thickness, Orientation, Hatch space and Density with mechanical characterization of the test parts. The optimum machining parameters were obtained by Grey relational analysis for the higher strength of the parts and confirmation tests were performed to make a comparison between the experimental results and developed model. The optimum levels of the parameter contributing to higher strength of the parts and density of the prototype are the end results of the paper, which is very useful information for machine designers as well as RP machine users.

## Keywords

*Rapid Prototyping; Stereolithography; Strength Analysis; Taguchi Method; Grey Relational Analysis; Optimization Techniques*

## Introduction

In today's manufacturing world, quality plays a vital important role. Quality can be defined as the fitness for the use or degree of customer satisfaction as provided by the product [1]. The product quality depends on the desired requirements of the intended functions in the various areas of application [2]. In the field of prototyping, the quality mainly depends upon the built parameters such as layer thickness, Orientation, Post processing time, Hatch Space, Hatch overcure, cure depth, which in turn is influenced by the mechanical and physical quality characteristics of the prototypes [3, 29]. These mechanical features of the prototypes are directly related to process parameters. In other words, the prototype quality depends on the machine process parameters. Solid freeform fabrication or additive manufacturing is a production process the physical prototype of which is created based on the concept of layer manufacturing technology. The invention of the technology has been preliminary fulfilled the engineering applications, especially for products which have complex shape and internal structure. Some additive manufacturing utilizations in industries include fabrication of mold and die [4, 5], producing of aircraft component prototype for aerodynamic analysis [6, 7], and making of full-size automobile instrument panels [8]. Among the various layered manufacturing processes, Stereolithography (SLA) is being recognized as an innovative technology, it still cannot be fully utilized in tooling applications since it lacks in part quality characteristics. The main objective is to analyze the strength of the SLA (Epoxy Resin) Component. One of the important applications of SLA process is rapid tooling in dies of Injection molding, pattern of casting. The Dies made through SLA process are subjected to high tension, compression and impact factor due to high injection pressure. In order to have higher number of injections without premature failure, the die should possess high tensile, flexural and impact strength [9]. Tensile Strength is crucial in the case of rapid tooling since the parts have to withstand pressures during the test of fitment and when they are used as die for injection moldings. Thus, work aims to study the strength and density of CIBSTOOL SL5530 Resin parts produced by SLA5000 Stereolithography machine and an efficient method for determining the optimal process parameters for multiple quality characteristics, through integrating

the grey theory with the taguchi method.

**Back Ground And Experimental Design**

Various process parameters affect the SL process quality. Schaub et al [10] identified more than fifty process parameters that induce errors and affect part accuracy. From Table 1, it is observed that layer thickness (Lt) hatch spacing (Hs) and orientation (O) are the most influencing process parameters on part quality characteristics. Lee et al [11], Jayanthi et al [12] and chockalingam et al [13] carried out extensive investigations on how the contribution of each process parameter on the part quality.

TABLE 1. PARAMETERS CONSIDERED FOR PARAMETRIC OPTIMIZATION OF SL PROCESS

Year	Author	Layer Thickness	Orientation	Hatch Spacing	Post curing time	Laser power	Scanning velocity	Over cure depth
1992	Jacobs	√	√	×	×	√	×	×
1997	Rahmate & Dickens	√	×	×	×	×	×	×
1997	Schaub et. al	√	√	×	×	×	√	×
2002	Harris et.al	√	×	×	×	×	×	×
2006	Chockalingam et.al	√	√	×	√	×	×	×
2009	Raju et al	√	√	√	×	×	×	×

√ - Parameters considered , × - Parameters not considered.

A standard approach for experimental design is to use the full factorial method, but which is time-consuming and more expensive, hence the Taguchi methods of experimental design provide a simple, efficient and systematic approach called fractional factorial method for minimizing the number of total experiment runs [14,15]. Taguchi technique is the most efficient problem solving tool which can improve the performance of the product, process, design and system with a significant slash in experimental time and cost. Taguchi technique increases the power of analysis of experimental data by complex analysis of variance and an efficient way to determine the optimum factor level [16-18]. Benefits of the S/N Ratio include increasing the factor weighting effect, decreasing mutual action, simultaneously processing the average and variation, and improving engineering quality. Depending on the required objective characteristics, different calculation methods can be applied as follows:

- where the objective optimal value is smaller, the smaller-the-Better (SB) method applies, such as in surface roughness and dimension accuracy error.

$$\eta = -10 \log \left[ \frac{1}{n} \sum_{k=1}^n y_k^2 \right] \dots \dots \dots (1)$$

- where the objective optimal value is larger, the larger-the-better (LB) method applies, such as in material removal rate and mechanical properties such as tensile, impact and flexural strength.

$$\eta = -10 \log \left[ \frac{1}{n} \sum_{k=1}^n \frac{1}{y_k^2} \right] \dots \dots \dots (2)$$

- where the objective optimal value is particular (preferable), the nominal-the-better (NB) method applies, such as in coating depth and others.

$$\eta = -10 \log \left[ \frac{1}{n-1} \sum_{k=1}^n (y_k - \mu)^2 \right] \mu = \frac{1}{n} \sum_{k=1}^n y_k \dots \dots \dots (3)$$

where  $\eta$  : signal-to-noise Ratio (S/N Ratio);  $y_k$ : the K-th result of the experiment; n: the repeated number of the K-th experiment;  $\mu$ : mean value of the experiment. After selecting optimal process parameter levels, the final step predicts and verifies the objective function. The predicted optimum value of the S/N ratio ( $\eta_{pred}$ ) is [19]:

$$\eta_{pred} = m + \sum_j^p [(m_{i,j})_{max} - m] \dots \dots \dots (4)$$

where  $(m_{i,j})_{max}$  is the S/N ratio of optimum level i of parameter j, m is the overall mean of the S/N Ratio and p is the number of parameters affecting the objective function [20].

The controlled parameters and their corresponding design levels are shown in Table 2 and the orthogonal array adopted in the experimental work is  $L_9$  as shown in Table 3 with larger the better for the mechanical part quality characteristics and smaller the better for the physical part quality characteristics.

TABLE 2. PARAMETER LEVELS FOR MAIN EXPERIMENT

Symbol	Response Parameter / Variable	LEVEL 1	LEVEL 2	LEVEL 3
A	Layer Thickness - $L_t$	0.075	0.10	0.125
B	Orientation - O	0°	45°	90°
C	Hatch Space - $H_s$	0.01	0.015	0.02

TABLE 3. DESIGN OF  $L_9$  ( $3^3$ ) ORTHOGONAL ARRAY WITH EXPERIMENTAL RESULTS AND S/N RATIO

Experi- mental Run	Control parameters			Experimental Value							
	$L_t$	O	$H_s$	Tensile Strength (N/mm <sup>2</sup> )	S/N Ratio	Flexural Strength (N/mm <sup>2</sup> )	S/N ratio	Impact Strength (J/m)	S/N ratio	Density analysis (Kg/m <sup>3</sup> )	S/N ratio
1	1	1	1	55.46	34.89	116.67	41.34	20.8	26.36	1.2345	-1.83
2	1	2	2	54.57	34.74	113.92	41.13	22	26.85	1.3855	-2.83
3	1	3	3	55.07	34.82	114.08	41.14	21.1	26.48	1.3235	-2.44
4	2	1	2	58.46	35.34	115.7	41.26	20.3	26.15	1.2405	-1.87
5	2	2	3	54.51	34.73	110.0	40.82	17.9	25.05	1.2395	-1.86
6	2	3	1	58.59	35.36	115.6	41.26	21.3	26.57	1.2255	-1.76
7	3	1	3	58.62	35.36	115.8	41.27	21.4	26.61	1.4055	-2.96
8	3	2	1	55.34	34.86	114.8	41.99	19.9	25.98	1.3450	-2.57
9	3	3	2	61.73	35.81	118.7	41.49	23.6	27.46	1.3568	-2.65

**Grey Analysis**

*Grey Relation Generating*

The grey theory investigates a system model with uncertain and insufficient information [21-23]. The gray relational analysis among sequence group requires that all sequences satisfy comparability conditions, for instance, non-dimension, scaling and polarization attributes. If comparability does not exist within sequence, the grey relationship generating approach can be adopted to transform the original sequence factor space into measurable space, generating a comparable sequence with three different comparability types as follows,

- The larger-the better (LB): the larger objective value is better and the property can be represented as the following equation,

$$x_i^*(k) = \frac{x_i^{(0)}(k) - \min x_i^{(0)}(k)}{\max x_i^{(0)}(k) - \min x_i^{(0)}(k)} \dots \dots \dots (5)$$

- The smaller-the-better (SB): the smaller objective value is better.

$$x_i^*(k) = \frac{\max x_i^{(0)}(k) - x_i^{(0)}(k)}{\max x_i^{(0)}(k) - \min x_i^{(0)}(k)} \dots \dots \dots (6)$$

- The nominal-the-better (NB): the value closer to the objective value OB is better,

$$x_i^*(k) = 1 - \frac{[x_i^{(0)}(k) - OB]}{\max\{\max x_i^0(k) - OB; OB - \min x_i^{(0)}(k)\}} \dots \dots \dots (7)$$

where  $x_i^*(k)$  is the value after Grey relation generating process and  $\min x_i^0(k)$ ,  $\max x_i^0(k)$  denotes the minimum and maximum of  $x_i^0(k)$  respectively. The grey relational grade in the grey relational analysis is defined as the relative degree between two sequences. Only one sequence  $x_0(k)$  selected as the reference sequence is called the localized grey relational grade, i.e., one sequence exists in the grey relational space  $\{P(X); \tau\}$ .

**Entropy Weighting**

Entropy weighting employs the entropy concept to determine the relative weighting factor for each attribute. Computing entropy value through the selected case effect for each attribute determines the uncertain deliverable degree of information for the entire decision making process. Then, comparing the entropy value for each attribute calculates the relative importance among all the attributes, or the relative weighting factor. The relative weighting factors obtained by entropy weighting apply evaluated attribute information among all selected cases, not including the artificial subjective factor of decision maker; hence, entropy weighting belongs to the objective-weighting factor. Entropy weighting is introduced as follows (24, 25):

- i) Compute each attributes summation value for all sequences,  $D_k$

$$D_k = \sum_{i=1}^m x_i(K) \dots \dots \dots (8)$$

- ii) Compute the normalization coefficient K,

$$K = 1/0.6487n \dots \dots \dots (9)$$

- iii) Find the entropy for the specific attribute,  $e_k$

$$e_k = K \sum_{i=1}^m w_s(z_i) \dots \dots \dots (10 a)$$

$$w_s(z_i) = z_i e^{(1-z_i)} + (1 - z_i) e^{z_i} - 1 \dots \dots \dots (10 b)$$

$$Z_i = \frac{x_i(K)}{D_k} \dots \dots \dots (10 c)$$

- iv) Compute the total entropy value, E:

$$E = \sum_{k=1}^n e_k \dots \dots \dots (11)$$

- v) Determine the relative weighting factor,  $\lambda_k$ .

$$\lambda_k = \frac{1}{n - E} |(1 - e_k)| \dots \dots \dots (12)$$

- vi) Using the normalization method, each attribute weight or quality characteristic, can be calculated as

$$\omega_j = \frac{\lambda_k}{\sum_{k=1}^n \lambda_i} \dots \dots \dots (13)$$

**Grey relation Grade**

The major calculation processes includes the following:

i) Endow the weighting factor: According to the grey relational generating data, the weighting factors of each attribute are given.

ii) After selecting the weighting factor, the following equation is computed

$$\Delta_{0i}(k) = |x_0(k) - x_i(k)| \dots \dots \dots (14)$$

Where  $i = 1, 2, \dots, m$ ,  $k = 1, 2, \dots, n$   $j \in i$

$x_0$  represents the weighting factor for each attribute; hence,  $x_0(k)$  and  $x_i(k)$  are the reference (ideal) sequence and the specific relative sequence respectively.

iii) Calculate the grey relational Grade  $\Gamma_j$  through the following equation

$$\Gamma_j = \frac{\Delta_{min} + \Delta_{max}}{\Delta_j + \Delta_{max}} \dots \dots \dots (15)$$

where  $\Delta_j = \frac{1}{n} \sum_{i=1}^n \Delta_{0i}(k)$  and  $\Delta_{min}, \Delta_{max}$  are constants as

$$\Delta_{min} = \forall j^{min} \in \forall k^{min} |x_0(k) - x_j(k)| \dots \dots \dots (16 a)$$

$$\Delta_{max} = \forall j^{max} \in \forall k^{max} |x_0(k) - x_j(k)| \dots \dots \dots (16 b)$$

The Table 4 shows the grey relational grade for each experiment using  $L_9$  orthogonal array. The higher grey relational grade represents that the corresponding experimental result is closer to the ideally normalized value. Experiment NO. 9 has the best multiple performance characteristics among nine experiments because it has the highest grey relational grade. In other words, optimization of the complicated multiple performance characteristics can be converted into optimization of a single grey relational grade. Since the experimental design is orthogonal, it is possible to separate out the effect of each built parameter on the grey relational grade at different levels. The mean of the grey relational grade for each level of the parameter is summarized as shown in the Table 5. The total mean of the grey relational grade for the nine experiments is computed and listed in Table 5. Figure 2 shows the grey relational grade graph for the levels of the parameters. Basically, the larger the grey relational grade, the better is the multiple performance characteristics.

TABLE 4 PRIORITY LIST OF WEIGHTED GREY RELATIONSHIP FOR MULTIPLE BUILDING QUALITY CHARACTERISTICS

No	Grey relationship generating				Grey relational analysis				Grey relational grade	
	TS	FS	IS	DA	Weighting via entropy method				$\Gamma_j$	Rank
					0.3538	0.1934	0.2016	0.2512		
1	0.1454	0.7667	0.5087	0.95	0.0514	0.1483	0.1026	0.2386	0.7550	4
2	0.0083	0.4506	0.7193	0.1111	0.0029	0.0871	0.0908	0.0279	0.6414	9
3	0.0776	0.4689	0.5614	0.4556	0.0275	0.0907	0.0945	0.1145	0.6777	7
4	0.5471	0.6552	0.4211	0.9167	0.1936	0.1267	0.0849	0.2303	0.7948	2
5	0	0	0	0.9222	0	0	0	0.2316	0.6481	8
6	0.5651	0.6437	0.5965	1	0.1999	0.1245	0.1202	0.2512	0.7772	3
7	0.5693	0.6667	0.6141	0	0.2014	0.1289	0.1238	0	0.7216	5
8	0.1150	0.5517	0.3508	0.3361	0.0406	0.1067	0.0707	0.0844	0.6698	6
9	1	1	1	0.2706	0.3538	0.1934	0.2016	0.0679	0.8853	1

TABLE 5 RESPONSE TABLE FOR THE GREY RELATIONAL GRADE

Symbol	Parameter	Grey relational grade			
		Level 1	Level 2	Level 3	Max-Min
A	Layer Thickness	0.6914	0.7400	0.7589	0.0675
B	Orientation	0.7571	0.6531	0.7800	0.1269
C	Hatch spacing	0.734	0.7738	0.5791	0.1947

Total mean grey relational grade = 0.7186

### Analysis Of Variance

Analysis of Variance (ANOVA) is a method of apportioning the variability of an output to various inputs [26]. The purpose of the analysis of variance is to investigate which built parameters significantly affect the quality performance characteristics [27, 28], which is accomplished by separating the total variability of the grey relational grades, which is measured by the sum of the squared deviations from the total mean of the grey relational grade, into contributions by each parameter and the error. First, the total sum of the squared deviations  $SS_T$  from the total mean of the grey relational grade  $\gamma_m$  can be calculated as

$$SS_T = \sum_{j=1}^p (\gamma_j - \gamma_m)^2 \tag{17}$$

where  $p$  is the number of experiments in the orthogonal array and  $\gamma_j$  is the mean grey relational grade for the  $j^{\text{th}}$  experiment. The total sum of the squared deviations  $SS_T$  which consists of the sum of the squared deviation ( $SS_a$ ) due to each built parameter and the sum of the squared error ( $SS_e$ ). The percentage contribution by each of the built parameters in the total sum of the squared deviations which can be used to evaluate the importance of the built parameter change on the performance characteristics. In addition, the Fisher's F-test can be used to determine which machining parameters have a significant effect on the performance characteristics [26]. The results of ANOVA for overall grey relational grade are shown in Table 6, which indicates that the orientation is the most significant built parameter which affects the multiple performance characteristics. Thus, the optimal built parameters are Layer thickness at level3, orientation at level 3 and Hatch space at level 2.

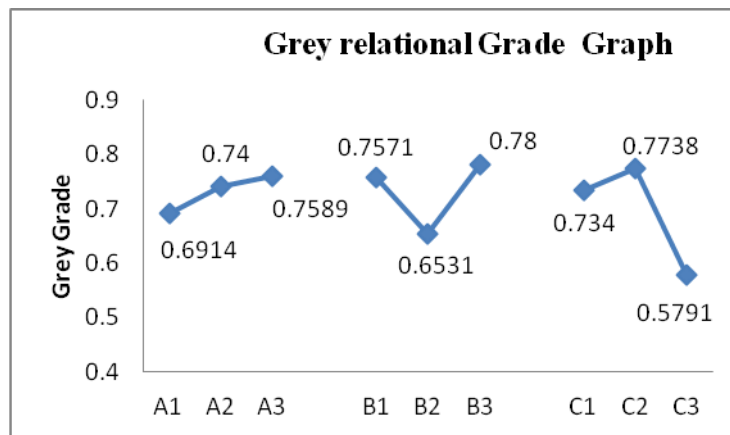


FIGURE 2: GREY RELATIONAL GRADE GRAPH

TABLE 6 PARAMETER VARIANCE AND CONTRIBUTION ANALYSIS FOR MULTIPLE QUALITY CHARACTERISTICS BASED

Parameter "i"	Sum of Squares	Degree of freedom	Mean sum of squares	F Statistics	F tabulated $F_{(0.25,2,2)}$	% of contribution	Significant
$L_t$	0.0072	2	0.0036			13.79	No
O	0.0274	2	0.0137	1.4694		52.49	Yes
$H_s$	0.0127	2	0.00635	5.5918*	3	24.33	No
Error	0.0049	2	0.00245	2.5918		9.38	
Total	0.0522	8	0.0261				

\*Significance at 75% confidence Level ( F Statistics > F Tabulated)

### Confirmation Experiment

After evaluating the optimal parameter settings, the final step is to predict and verify the enhancement of the quality characteristics using the optimal parametric combination. The estimated Grey relational grade  $\gamma$  predicted using the optimal level of the design parameters can be calculated as:

$$\gamma_{Predicted} = \gamma_m + \sum_{i=1}^q (\bar{\gamma}_j - \gamma_m) \dots \dots \dots (18)$$

where  $\gamma_m$  is the total mean Grey relational Grade,  $\bar{\gamma}$  is the mean Grey relational grade at the optimal level and  $q$  is the number of the main design parameters that affect the quality characteristics[2]. Based on the equation 18, the estimated grey relational grade using the optimal built parameters can be obtained. The Table 7 indicates the confirmation experiment using the optimal parameter settings.

TABLE 7 RESULTS OF CONFIRMATION TEST

	Initial process parameters	Optimal machining parameters	
		Prediction	Experiment
Factors Level	A1/B1/C1	A3/B3/C2	A3/B3/C2
Tensile Strength	55.46		61.73
Flexural Strength	116.67		118.7
Impact strength	20.8		23.6
Density analysis	1.2345		1.3568
Overall Grey relational grade	0.7550	0.8755	0.8853

Improvement in Grey relational grade = 0.1303

The Tensile strength is improved from 55.46 to 61.73 N/mm<sup>2</sup>, the flexural strength from 116.67 to 118.7 N/mm<sup>2</sup> and the impact strength from 20.8 to 23.6 J/m. It is clearly shown that multiple performance characteristics in the built process are greatly improved through this study.

## Conclusions

The use of an orthogonal array with grey relational analysis to optimize the built parameters with multiple performance characteristics has been reported in the paper. The grey relational analysis of the experiment results of tensile, flexural and impact strength can convert optimization of the multiple performance characteristics into the optimization of the single performance characteristics called the grey relational grade. The study has concentrated on the application of Taguchi method coupled with Grey relation analysis for solving multi criteria optimization problem in the field of rapid prototyping process. Experimental results have shown that the mechanical strength of the Stereolithography parts are enhanced by using Grey based Taguchi method. The optimal combination of process parameters based on multiple quality characteristics are A3/ B3/ C2 i.e., 0.125 Layer thickness, 90° Orientation and 0.015 hatch spacing.

## REFERENCES

- [1] L.Kukielka, Journal of Mechanical Technology, 19,1989, PP: 319-356.
- [2] Hakan Aydin, Ali Bayram, Ugur Esme, Yigit Kazancoglu and Onur guven, Application of Grey relation analysis and Taguchi method for the parametric optimization of Friction Stir Welding Process, Materials and Technology , 44(4), PP:205-211 (2010).
- [3] B.S.Raju, U Chandra Shekar , D N Drakshayani, Determining the influence of layer thickness for Rapid prototyping with Stereolithography (SLA) process,(IJEST 10-02-07-142), International Journal of Engineering science and Technology, Vol.2(7), 3199-3205 (2010).
- [4] J.Y.Jeng and Lin, M.C. Mold fabrication and modification using hybrid processes of selective laser cladding and milling, Journal of Materials Processing Technology, Vol 110, 98-103 (2001).
- [5] Y.Song, Y.Yan, R.Zhang, D.Xu and F.Wang, Manufacture of the die of an automobile deck part based on rapid prototyping and rapid tooling technology, Journal of Materials Processing Technology, vol 120, 237-242 (2002).
- [6] Zhu, W., Li, D., Zhang, Z., Ren, K., Zhao, X., Yang, D., Zhang, W., Sun, Y. and Tang, Y. Design and fabrication of Stereolithography-based aero elastic wing models. Rapid Prototyping Journal, Vol 17, 298-307 (2011).
- [7] Kroll, E. and Artzi, D, Enhancing aerospace engineering students learning with 3D printing wind-tunnel models, Rapid Prototyping Journal. Vol17, 393-402 (2011).

- [8] Wohler's, T, State of the Industry Annual Worldwide Progress Report on Additive Manufacturing. Wohler's Associates, Colorado, U.S.A., pp.42 (2009).
- [9] B.S.Raju , U Chandrasekhar ,K Venkateswarlu, D N Drakshayani, Establishment of process model for rapid prototyping technique (Stereolithography) to enhance the part quality by Taguchi method, *Procedia Technology* 14, PP380-389 (2014) Elsevier, Science Direct. DOI :10.1016/j.protcy.2014.08.049.
- [10]Schaub, D. A., Chu, K.R., Montgomery, D. C, "Optimizing Stereolithography Throughput", *Journal of Manufacturing Systems*, Vol. 6 No.4 , pp. 290-303 (1997).
- [11]Lee, S.H., Park, W. S., Cho, H.S., Zhang, W., Leu, M.C, A neural network approach to the Modeling and Analysis of Stereolithography Process, *Proc. Institution of Mechanical Engineers*, Vol. 215, Part B, pp. 18 – 27 (2001).
- [12]Jayanthi, S., Keefe, M., Gargiulo, E.P, "Studies in Streolithiography: Influence of Process Parameters in Photopolymer model" In *Proc. of the Solid Freeform Fabrication Symposium, U.S.A, 1995*, pp 170-180.
- [13]K Chockalingam, N.Jawahar, U Chandrasekhar and K N Ramanathan, Establishment of process model for part strength in Stereolithography, *Journal of Materials Processing Technology*, Vol 208 , pp 348-365 (2008).
- [14]Yang W H and Tarang Y S, Design optimization of cutting parameters for turning operations based on the Taguchi method, *Journal of Material Processing Technology*, Vol 84, PP:122-129 (1998).
- [15]Tosun N, Cogun C and Gul T, A study on kerf and material removal rate in wire electrical discharge machining based on the Taguchi method, *Journal of Materials processing Technology*, Vol 152, pp 316-322 (2004).
- [16]Kim S J, Kim K S and Ho J, Optimization of manufacturing parameters for a brake lining using Taguchi method, *Journal of Materials processing Technology*, Vol 136, pp 202-208 (2003).
- [17]Syracos G P , Die casting process optimization using Taguchi methods, *Journal of Materials processing Technology*, Vol 135, pp 68-74 (2003).
- [18]Ghani J A, Choudhury I A and Hassan H, Application of Taguchi method in the optimization of end milling parameters, *Journal of Materials processing Technology*, Vol 145, pp 84-92 (2004).
- [19]Phadke,M.S., *Quality Engineering using Robust Design*, Prentice Hall, Englewood cliffs, NJ, 1989.
- [20]Kuo-Wei Lin and Che-chung Wang, Optimizing Multiple quality characteristics of WEDM via Taguchi method-based grey analysis for Magnesium alloy, *Journal of C.C.I.T*, vol 39, 23-33 (2010).
- [21]Lin,J.L., Wang,K.S., Yan,B.H., and Tarang, Y.S., Optimizing of the multi-response process by taguchi method with grey relational analysis, *The Journal of Grey system*, Vol 10, No.4, pp.355-370,1998.
- [22]Pan,L.K, Wang,C.C., Wei,S.L., Sher,H.F., Optimizing multiple quality characteristics via Taguchi method-based grey analysis, *Journal of Materials processing Technology*, Vol.182, Issue 1-3, pp.107-116, (2007).
- [23]Wang,C.C., Lin,T.W., Hu,S.S., Optimizing the rapid protoyping process by integrating the taguchi method with the grey relational analysis, *Rapid protoyping journal*, Vol 13, N0 5, PP-304-315 (2007).
- [24]H.rowlands, J.Antony, G.Knowles, *The TQM Magazine*, 12, 78-83 (2000).
- [25]Roy,R.K., *Design of experiments using the taguchi approach: 16 steps to product and process improvement*, in: Wiley Interscience, New York, (2001).
- [26]R.A.Fisher, *Statistical Methods for Research Worker*, Cosmo Publications, New Delhi (2005)
- [27]S Datta, A Bandyopadhyay, P K Pal , *International Journal of Advanced Manufacturing Technology*, Vol 39, pp1136-1143 (2008).
- [28]U Esme, M Bayramogulu, Y Kazangoglu, *Materials and Technology*, Vol 43, pp: 143-149 (2009).
- [29]Raju B S, U Chandra Shekar , D N Drakshayani, Optimization studies on improving the strength characteristic for parts made of photosensitive polymer, *Journal Institute of Engineers, India -Springer, Series D* ,Vol. 94 (1), PP 35-41 (2013) DOI: 10.1007/s40033-013-0020-6.



**Prof. Raju B S** working as associate professor in the Department of Mechanical Engineering, REVA ITM, having 15 national and International journal paper publication and morethan 45 national and International conference publication in the area of Rapid prototyping,, Operration research, Optimization Techniuqe, Surface coatings, UIT treatment of weldmets etc.

**Dr. U.Chandra sekhar**, an Former Scinetist G and Additional Director, GTRE, DRDO and Presently working as Director, Institution of Engineers (India), Gachibowl, Hyderabad-32.He has more 50 plus publication in the field of rapid prototyping.

**Drakshayani D N** , Professor, Department of Mechanical Engineering, Sir.M.VIT, Bangalore, Karnataka. India.

# Experimental Study on Mechanical Properties of Aluminium Metal Matrix Composites (AA 6061 Reinforced with MOS<sub>2</sub>)

E. Subba Rao<sup>1</sup> and N.Ramanaiah<sup>2</sup>

<sup>1</sup>Associate Professor, Department of Mechanical Engineering, Loyala Institute of Technology and Management, sattenapalli, Guntur, Andhra Pradesh, India

<sup>2</sup>Professor, Department of Mechanical Engineering,

A. U. College of Engineering (A), Andhra University, Visakhapatnam-530 003, Andhra Pradesh, India.

<sup>1</sup>esrlitam@gmail.com; <sup>2</sup>n.rchetty1@gmail.com

## Abstract

The present study is aimed at evaluating the mechanical properties of aluminium metal matrix composite (AMMC). An effort is made to enhance the mechanical properties like hardness, tensile strength, yield strength, % of elongation of AMMCs by reinforcing AA6061 matrix with Molybdenum di sulfide (MOS<sub>2</sub>) particles. AMMCs were made, AA6061 as matrix material and MOS<sub>2</sub> as reinforcement material, through stir casting method. AMMCs with varying percentage by different wt. %, 1%, 2 %, 3%, 4%,5% MOS<sub>2</sub> were fabricated. A systematic study of the matrix metal and AMMCs is done to evaluate the mechanical properties (hardness, yield strength and tensile strength) in as cast and heat treated condition. It was observed that in comparison to the matrix metal, the precipitation kinetic was accelerated by adding the MOS<sub>2</sub> particles. It was noticed that, mechanical properties are increasing with the increase in wt. % of the reinforcement up to 4% MOS<sub>2</sub> further addition there is a diminution in both the conditions (as cast and cold rolling followed by heat treatment condition). It was also thought-out that 4% MOS<sub>2</sub> composite shows better mechanical (hardness, yield strength and tensile strength) properties and low % of elongation than all other compositions in both the conditions. Optical microscopy and Scanning electron micrographs were carried out to authenticate the mechanical properties of the matrix metal and AMMCs.

## Keywords

AA6061; AMMC; MOS<sub>2</sub> Particles; As Casted; Cold Rolling Followed By Heat Treatment; Microstructure; SEM

## Introduction

Composites are engineered or naturally occurring materials made from two or more constituent materials with significantly different physical or chemical properties that remain separate and distinct within the finished structure. The bulk material forms the continuous phase that is the matrix (e.g.,metals, polymers)and the other acts as the discontinuous phase that is the reinforcement (e.g. ,ceramics, fibers, whiskers, particulates). While the reinforcing material as usually carries the major amount of load &the matrix enables the load transfer by holding them together [1]. Composite materials are gaining wide spread acceptance due to their characteristics of behavior with their high strength to weight ratio [2].The interest in material matrix composites (MMCs) is due to the relation of structure to properties such as specific stiffness or specific strength. Material matrix composites are being increasingly used in aerospace and automobile industries owing to their enhanced properties such as elastic modulus, hardness, tensile strength at room and elevated temperatures, wear resistance combined with significant weight savings over and reinforced alloys [3, 4]. The material matrix composite can be reinforced with particles and fibers. However, the biggest interest in composite materials is observed for those reinforced with hard ceramic particles due to the possibility of controlling their mechanical properties.

Mechanical properties were affected by selection of the volume fractions, size, and distribution of the reinforcing particles in the matrix [5].They are used more often, compared with the composite materials of other metals, due to the broad range of their properties and also due to the possibility of replacing the costly and heavy elements made

from the traditionally used materials [6, 7]. Metal matrix composites reinforced with particles tend to offer enhancement of properties processed by conventional routes [8].

AMMC are the competent material in the industrial world. Due to its excellent mechanical properties it is widely used in aerospace, automobiles, marine etc. [9]. The aluminium matrix is getting strengthened when it is reinforced with the hard ceramic particles like B<sub>4</sub>C, SiC, MOS<sub>2</sub> and Al<sub>2</sub>O<sub>3</sub> etc. Aluminium alloys are still the subjects of intense studies, as their low density gives additional advantages in several applications. These alloys have started to replace cast iron and bronze to manufacture wear resistance parts. The alloys primarily utilized today in construction of aircraft structures, such as wings and fuselages, more commonly in homebuilt aircraft than commercial or military aircrafts.

Aluminum hybrid metal matrix composites show better improvement in hardness with the increasing in percentage of reinforcement whereas decrease in density. (10). Mechanical properties (hardness, tensile strength and yield strength) of hybrid composites were increased with increasing Wt. % addition of reinforcements (11). Aluminium alloy AA6061 is available in a wide range of structural shapes, as well as sheet and plate products. This alloy has good weldable characteristics [12]. Aluminium is also ubiquitous element and one of the trace elements with moderate toxic effect on living organisms[13]. Hence the desire in the engineering community to develop a new material with greater mechanical properties, without much compromising on the strength to weight ratio led to the development of the metal matrix composites[14, 15].

A limited research work has been reported on AMMCs reinforced with MOS<sub>2</sub> due to higher raw material cost and poor wetting. MOS<sub>2</sub> is a robust material having excellent chemical and thermal stability, high hardness (HV=30 Gpa) and low density (2.52g/cm<sup>3</sup>) and it is used for manufacturing bulletproof vests, armor tank etc. Hence, MOS<sub>2</sub> reinforced aluminium matrix composite has gained more attraction with low costing route [16].

## Materials and Methods

### Materials

AA6061 is used as matrix metal and Molybdenum di sulphide (MOS<sub>2</sub>) powder of size 3-5 mesh as reinforcement material. The chemical composition of AA6061 and MOS<sub>2</sub> powder is shown in table.1 and table 2 respectively.

TABLE 1. COMPOSITION OF AA6061 MATRIX METAL

Ele	Cu	Mg	Si	Fe	Mn	Zn	Ti	Cr	Al
%	0.19	0.82	0.67	0.19	0.06	0.03	0.07	0.08	Rem

TABLE 2. COMPOSITION OF MOS<sub>2</sub>

Elements	MO	S
%	59.94	40.06

### Experimental Work

The simplest and the most cost effective method of liquid state fabrication is stir casting [17]. In this work stir casting technique is employed to fabricate, which is a liquid state metal in which a dispersed phase (reinforcement particulates) is mixed with a molten metal by means of stirring. The matrix AA6061 was melted at 700°C in an electric furnace. At this high temperature magnesium ribbons were added into the molten alloy to increase the weldability. An appropriate amount (1% of the weight of base metal) of MOS<sub>2</sub> powder was preheated (3500C) and then added slowly to the molten aluminium alloy. Simultaneously, the molten metal was stirred thoroughly at a constant speed of 300 rpm with a stirrer for a period of 15 min. For a evenly dispersing MOS<sub>2</sub> particles in the molten aluminium alloy the high temperature AMMC was poured into the preheated (4000C) cast iron mould. The same procedure was followed to get the AMMC's of different wt. %, 1%, 2%, 3%, 4% and 5% (having dimensions 300mmx300mmx6mm) the experimental setup is shown in Fig:1.

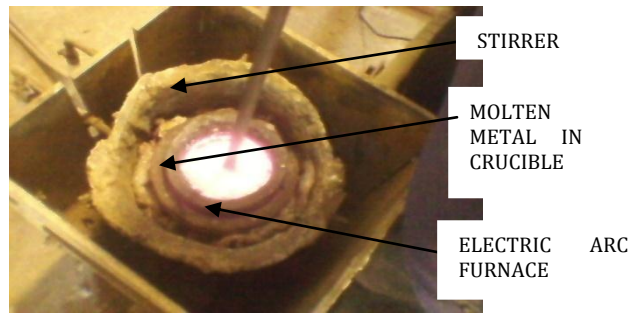


FIGURE 1 MOLTEN METAL IN THE FURNACE

### *Treatment of AMMC*

Fabricated composite was divided into equal parts of size 150x150x 6mm by mechanical cutting and are used for studying the mechanical properties in both the conditions (as cast and cold rolling followed by heat treatment).

#### *As Cast*

The fabricated specimens (150x150x6) were proposed to test for mechanical properties without any treatment.

#### *Cold Rolling Followed by Heat Treatment (CR & HT)*

The composite plate thickness was reduced by 10% through rolling process using a rolling mill. AMMC plates were solunized at 520°C for 1Hr and water quenched then the specimen are artificially aged at 180°C for a period of 12Hrs followed by air cooling.

### *Testing of AMMC*

The fabricated specimens were proposed to test for mechanical properties like hardness, tensile strength, yield strength and % of elongation.

#### *Hardness Test*

Hardness measurements were carried out on the matrix metal and composite samples by using standard Vickers hardness test machine. Vickers hardness measurements were carried out in order to investigate the influence of particulate weight fraction on the matrix hardness.

#### *Tensile Testing*

The specimens were machined to get dog boned structure as per ASTM E-8 standards. Test was carried out on a computerized UTM (TUE-C-600 Model Machine). The tensile test specimens are as per ASTM E-8 as shown in Fig: 2

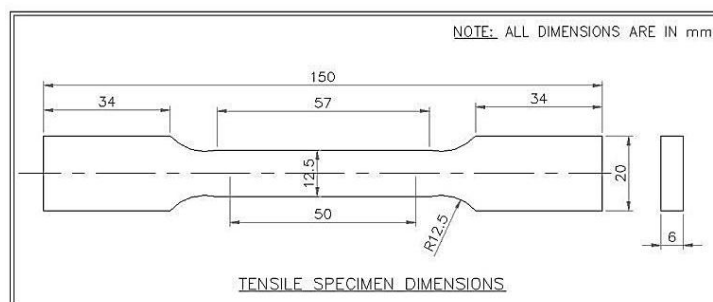


FIGURE 2 TENSILE TEST SPECIMEN AS PER ASTM –E8

### *Microstructure of AMMC*

Microscopic analysis of the matrix metal and composite samples is performed by optical microscopy and Scanning electron microscopy. An Image analyzer was used to examine the distribution of the reinforcement particles within the aluminum matrix. The mechanical properties of any particle reinforced metal matrix composites depend on the particle distribution, particle size, particle flaws, surface irregularities and particle matrix bonding. It is therefore,

necessary to conduct a microscopic analysis on the new material in order to gain better understanding of its micro structural characteristics. The polished specimens were cleaned with acetone and etched with (Methanol (25ml) + Hydrochloric acid (25ml) + Nitric Acid (25ml) + Hydrofluoric acid 1 drop) solution.

**Results & Discussions**

*Hardness*

The tests revealed that, the hardness of the composite specimen is increased gradually with increase in the wt. % of MOS<sub>2</sub> powder incorporated in the metal matrix. The same thing was observed in hybrid composites (10 and 11). Table 3 shows hardness (VHN) of the composite at various percentage of reinforcement (MOS<sub>2</sub>) in both the conditions (as cast and cold rolled followed by Heat treatment). Fig: 3 show the hardness all composites (1%, 2%, 3%, 4% & 5% of MOS<sub>2</sub>) in both the conditions. Cold rolled followed by Heat treated condition composite shows better hardness values than as cast condition and out of all conditions and compositions, 4% of MOS<sub>2</sub> composite shows better hardness.

TABLE 3. HARDNESS (VHN) OF THE COMPOSITE AT VARIOUS PERCENTAGE OF REINFORCEMENT (MOS<sub>2</sub>) IN BOTH THE CONDITIONS (AS CAST AND COLD ROLLED FOLLOWED BY HEAT TREATMENT)

Condition \ %MOS <sub>2</sub>	As cast	Cold Rolling
1%	65	72.0
2%	89	92.0
3%	101	102.0
4%	109	110.0
5%	91	95.00

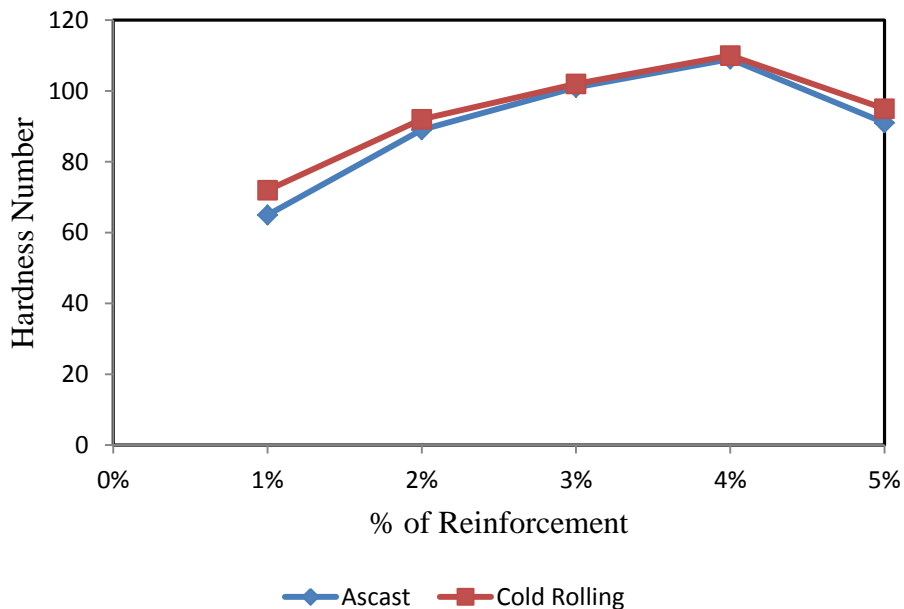


FIGURE 3 HARDNESS (VHN) OF THE COMPOSITE AT VARIOUS PERCENTAGE OF REINFORCEMENT (MOS<sub>2</sub>) IN BOTH THE CONDITIONS (AS CAST AND COLD ROLLED FOLLOWED BY HEAT TREATMENT)

*Mechanical Properties (Tensile Strength, Yield Strength & % of Elongation)*

The tests revealed that, the tensile strength of the composite specimen increased gradually with increase in the wt. % of MOS<sub>2</sub> powder incorporated in the metal matrix. The same thing was observed in hybrid composites (11). Fig.4

shows the tensile strength of all composites (1%, 2%, 3%, 4% & 5% of  $\text{MOS}_2$ ) in as cast, and cold rolled followed by heat treatment condition. Out of all, the cold rolled followed by heat treatment condition composite shows better tensile strength values than all cast condition. 4% of  $\text{MOS}_2$  composite made with cold rolling followed by heat treatment shows better mechanical properties than all other compositions. Similar trend was observed for yield strength (Fig.5).

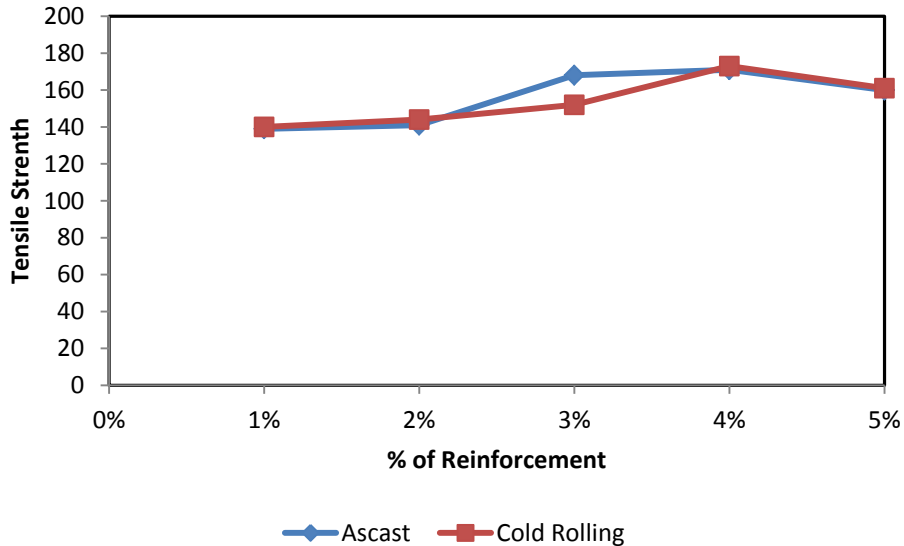


FIGURE 4 TENSILE STRENGTH OF COMPOSITES (1%, 2%, 3%, 4% & 5% OF  $\text{MOS}_2$ ) IN AS CAST AND COLD ROLLED FOLLOWED BY HEAT TREATMENT CONDITION

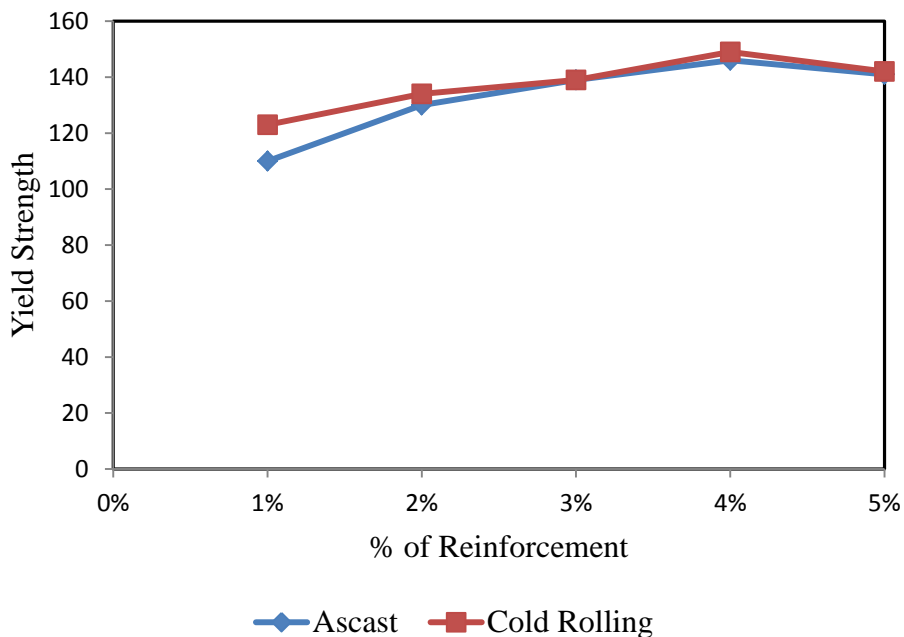


FIGURE 5 TENSILE STRENGTH OF COMPOSITES (1%, 2%, 3%, 4% & 5% OF  $\text{MOS}_2$ ) IN AS

#### ***Cast and Cold Rolled Followed by Heat Treatment Condition***

Where as the percentage of elongation of the composites are decreased gradually with increase in the wt. % of  $\text{MOS}_2$  powder incorporated in the metal matrix. Fig. 6 shows the percentage of elongation of all composites (1%, 2%, 3%, 4% & 5% of  $\text{MOS}_2$ ) in both the conditions. Composites made with cold rolling followed by heat treatment shows the lower percentage of elongation values than as cast condition. Out of all 4% of  $\text{MOS}_2$  Composite shows lowest % elongation than all other composites.

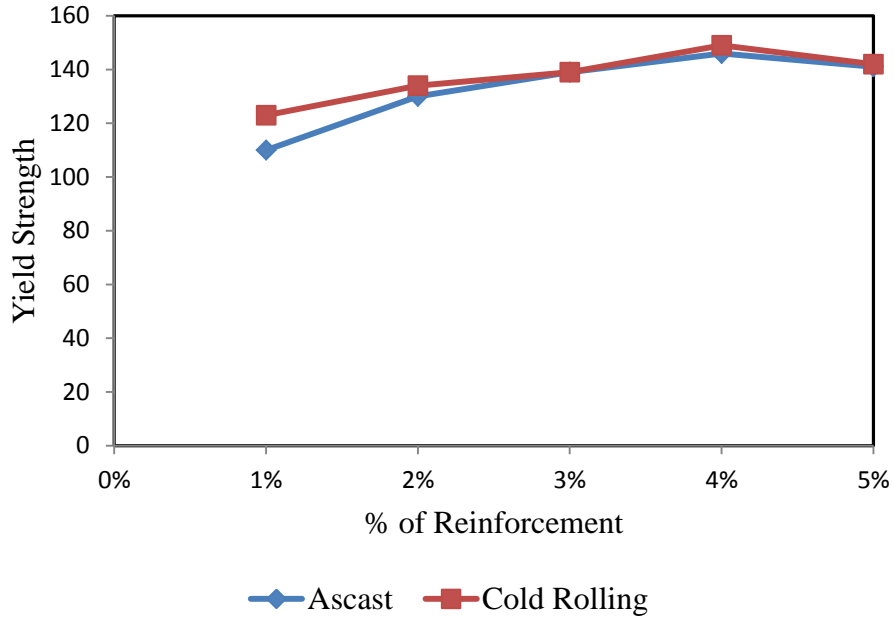


FIGURE 6 THE PERCENTAGE OF ELONGATION OF AS CASTED AND COLD ROLLED FOLLOWED BY HEAT TREATED AMMCS

**Micro Structure**

The morphology, density, type of reinforcing particles and its distribution have a major influence on the properties of particulate composites [1]. The specimens were prepared for microstructure analysis by thoroughly polishing and etching. Then the specimens were observed under an optical microscope and SEM for studying the microstructure.

Micrograph of the matrix metal (AA6061) in T6 temper is shown in Fig. 7a. It shows that numbers of Mg<sub>2</sub>Si articles present in artificially aged (T6) alloy and shows columnar without reinforcement and significant grain refinement was noticed when reinforced material (MOS<sub>2</sub>) were added to the matrix metal (Fig. 7b-e) in as cast condition.

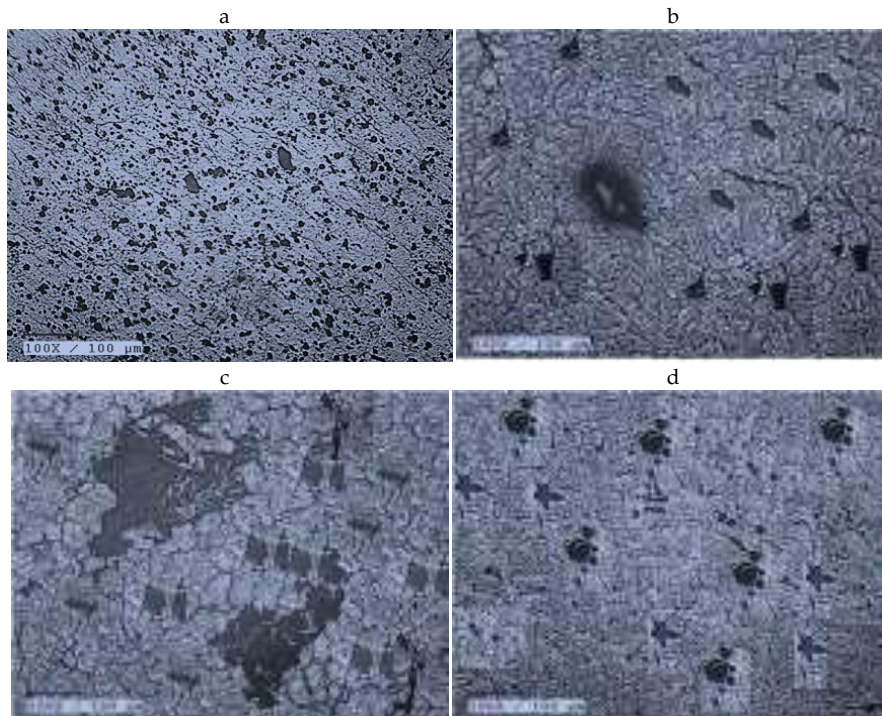


FIGURE 7.MICROGRAPHS OF (A) MATRIX METAL-T6 (B) 3% MOS<sub>2</sub> CAST COMPOSITE, (C) 4% MOS<sub>2</sub> CAST COMPOSITE AND D. 5% MOS<sub>2</sub> CAST COMPOSITE

Micrograph of the cold rolling followed by heat treatment composite is shown in the Fig. 8a-c. It shows number of  $Mg_2Si$  and  $MOS_2$  particles present and significant grain refinement was noticed when reinforced material ( $MOS_2$ ) were added to the matrix metal.

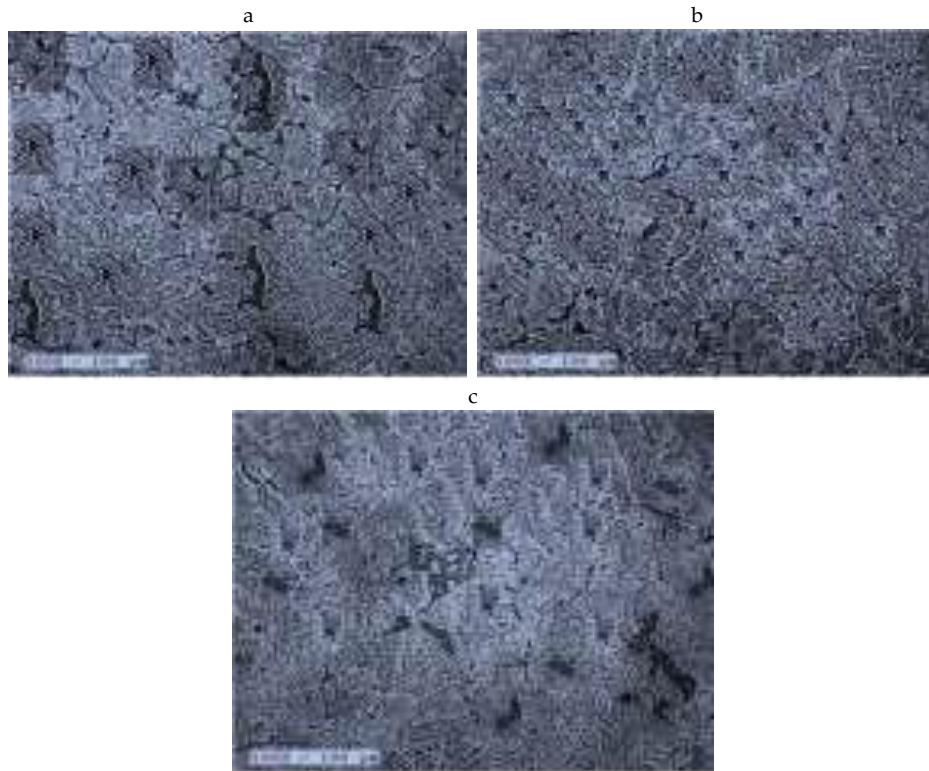


FIGURE 8 MICROGRAPHS OF (A) 3%  $MOS_2$  COLD ROLLING FOLLOWED BY HEAT TREATMENT COMPOSITE, (B) 4%  $MOS_2$  COLD ROLLING FOLLOWED BY HEAT TREATMENT COMPOSITE AND (C) 5%  $MOS_2$  COLD ROLLING FOLLOWED BY HEAT TREATMENT COMPOSITE

In Fig. 9b and c, small  $MOS_2$  particles are clearly visible, while almost no fine  $MOS_2$  particles are visible in the cast composite (the particles appear white in the SEM images due to charging of the nonconductive  $MOS_2$ ). Comparing the grain structure of the composite there is some grain refinement over the matrix material (Fig.9a). While complete quantitative data were difficult to obtain from the matrix material, columnar grains are clearly visible.

Conversely, the microstructure of the composite has much smaller grains. Fig: 9.c. shows a fine with many smaller grains predominantly near  $MOS_2$  particles. With the observed dispersion of fine  $MOS_2$  particles throughout the matrix in the cold rolling followed by heat treatment, it is possible that the high number of potential heterogeneous nucleation sites could give rise to a further refined grain structure. However, in the as cast composite (Fig.9b), there are large grains are observed.

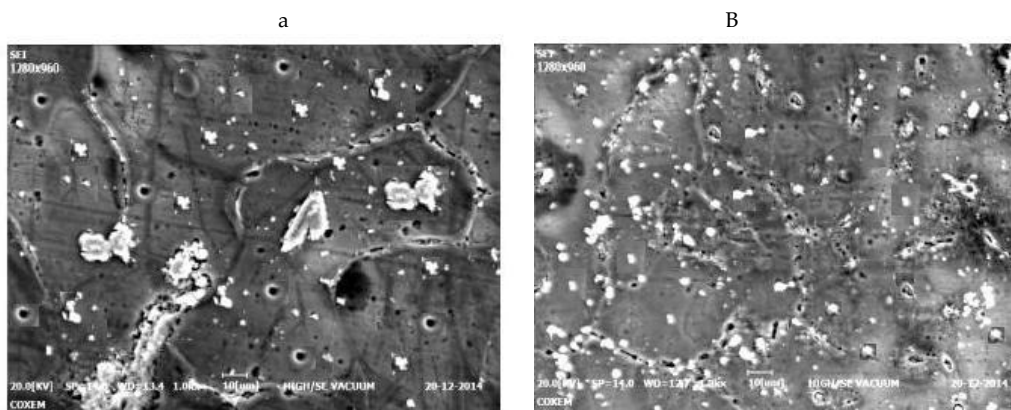


FIGURE 9 SEM MICROGRAPHS OF (A) MATRIX METAL (B) AS CAST (AA6061+  $MOS_2$ )COMPOSITE AND (C) COLD ROLLING FOLLOWED BY HEAT TREATED (AA6061+  $MOS_2$ )COMPOSITE

## Conclusions

The AA6061-MOS<sub>2</sub> composites of combinations 1%, 2%, 3%, 4% & 5% were produced through stir casting method. The mechanical properties of the composite of as cast and cold rolling followed by heat treatment were evaluated and compared matrix material and observed the distribution of reinforcements (precipitates) are homogenously distributed. The following conclusions are made from the study.

1. AA6061-MOS<sub>2</sub> composites AMMCs (AA6061/MOS<sub>2</sub>) were successfully fabricated by stir casting method.
2. The mechanical properties of 4% MOS<sub>2</sub> cold rolling followed by heat treatment AMMC showed better value than all other composites.
3. Out of all the conditions, cold rolling followed by heat treatment of 4% of MOS<sub>2</sub> shows better yield and tensile strength but lower % of elongation.
4. Optical micrographs and SEM micrographs revealed that the MOS<sub>2</sub> particles were well distributed in the Aluminium matrix with cold rolling followed by heat treatment condition.

## REFERENCES

- [1] Prashant Sharma, Determination of Mechanical Properties of Aluminium Based Composites International Journal on Emerging Technologies. 3(1): 157-159(2012), ISSN No. (Print): 0975-8364
- [2] Pai, B.C., T.P.D. Rajan and R.M. Pillai, 2004. Aluminium matrix composite castings for automotive applications. Ind. Foundry J., 50: 30-39.
- [3] A. Chennakesava Reddy and Essa Zitoun Indian Journal of Science and Technology Vol. 3 No. 12 (Dec 2010) ISSN: 0974- 68 46.
- [4] B. Neitzel, M. Barth, M. Matic, "Weight Reduction of Discs Brake Systems with the Utilization of New Aluminum Material", SAE Technical Paper Series, 940335, Warrendale, PA, USA.
- [5] R. Dwivedi, "Development of Advanced Reinforced Aluminum Brake Rotors", SAE Technical Paper Series, 950264, Warrendale, PA, USA, 1995, 8 p.
- [6] G. Mrówka-Nowotnik, J. Sieniawski, M. Wierzbika Analysis of intermetallic particles in AlSi1MgMn aluminium alloy, Journal of Achievements in Materials and Manufacturing Engineering 20 (2007) 155-158.
- [7] A. Wodarczyk-Fligier, L.A. Dobrzaski, M. Adamiak Influence of heat treatment on properties and corrosion resistance of Al-composite, Journal of Achievements in Materials and Manufacturing Engineering 21/1 (2007) 55-58.
- [8] L.A. Dobrzaski, A. Wodarczyk, M. Adamiak, Composite materiale based on EN AW-Al Cu4Mg1(A) aluminium alloy reinforced with the Ti(C,N) ceramic particles, Materials Science Forum 530-531 (2006) 243-248].
- [9] Mohanty RM, Balasubramanian K, Seshadri SK. Boron carbide-reinforced aluminium 1100 matrix composites: fabrication and properties. Material Science Eng. A 2008; 498:42-52]
- [10] Ch. Shoba, N. Ramanaiah, D. Nageswara Rao, Aging behavior of aluminium hybride metal matrix composites, Materials Science an Indian journal, Vol.10 issue11, 2014 484-489
- [11] Bhargavi Rebba and N. Ramanaiah, Investigations on Mechanical Behaviour of B4C and MOS<sub>2</sub> Reinforced AA2024 Hybrid Composites, Journal of Manufacturing Science and Production, Oct, 2015, DE GRUYTER
- [12] Feng YC, Geng L, Zheng PQ, Zheng ZZ, Wang GS. Fabrication and characteristic of Al-based hybrid composite reinforced with tungsten oxide particle and aluminum borate whisker by squeeze casting. Materials& Design 2008; 29: 2023-6.
- [13] Ibrahim, I.A., F.A. Mohamed, E.J. Lavernia, 1991. Metal matrix composites-a review. J. Mater. Sci., 26: 1137-1157. DOI: 10.1007/BF00544448.
- [14] Buraimoh, A.A., S.A. Ojo, J.O. Hambolu and S.S. Adebisi, 2012. Aluminium chloride exposure had no effects on the epididymis of wistar rats. Am. Med.J., 3: 210-219. DOI: 10.3844/amjsp.2012.210.219.
- [15] Sinclair, I. and P.J. Gregson, 1997. Structural performance of discontinuous metal matrix composites. Mater. Sci. Technol., 3: 709-726. DOI: 10.1179/026708397790290254;

- [16] Sannino, A.P. and H.J. Rack, 1995. Dry sliding wear of discontinuously reinforced aluminum composites: Review and discussion. *Wear*, 189: 1-19. DOI: 10.1016/0043-1648(95)06657-8.
- [17] Kerti I, Toptan F. Microstructural variations in cast MOS<sub>2</sub>-reinforced aluminium matrix composites (AMCs). *Mater.Lett.*2008; 62:1215–8. 4.
- [18] Hashim J., Looney L., and Hashmi M.S.J., 1999, Metal Matrix Composites: Production by the Stir Casting Method, *Journal of Material Processing and Technology*, 92, pp.17.

# A Method to Ensure Long-term Adhesion Quality of Al-LDPE-Al Hybrid Sandwich Panels

A.R.Torun\*

Zahit Alüminyum San. ve Tic. A.Ş. Hacı Sabancı Organize Sanayi Bölgesi Oğuz Kağan Köksal Cad. No:5 Sarıçam / Adana / Turkey

\* refahtorun@gmail.com

## *Abstract*

The adhesion problem of aluminum polyethylene sandwich panels is analyzed within the scope of this study. The theoretical necessary adhesion value for maximum shear stress is calculated. A selected area of the panel is scanned with a peeling test. The set limit value of adhesion led to no customer claims within the observed period of six months. The condition of machine elements and the recycled material quality of polyethylene are also determined.

## *Keywords*

*Sandwich Panel; Metal Polymer Adhesion; Aluminum; Polyethylene*

## **Introduction**

Metal-polymer-metal sandwich panels are widely used in civil engineering applications and gaining more and more importance for the transportation and automotive applications. Intensive research efforts can be seen in the literature to eliminate the use of adhesives between metal and polymer parts. There are such methods to bind an aluminum alloy and high density polyethylene with a friction-stir welded joint [1]. Also the joint of fiber reinforced thermoplastic polymer and metal structures were specifically evaluated [2]. A review and evaluation of various polymer-metal-hybrid approaches with a direct (adhesive-free) adhesion between metal and injection-molded thermoplastics was given [3].

There is the possibility of polymer modifications to enhance the adhesion between polymer and metal. Pesetshii et al. describe the functionalization of polyethylene with increasing adhesion to copper, steel and aluminum [4]. Energetic ion irradiation was successfully applied to improve the adhesion of polyethylene naphthalate films to deposited copper layers [5].

Al-LDPE-Al hybrid sandwich panels are produced in industrial scale and being increasingly used to cover outer surfaces of modern buildings. These panels may have a mirror finish to reflect the sunlight or dark colors to absorb the radiation, which can reduce the overall energy consumption of a building in a warm or cold climate zone. Beside the wide possibility of colors and visual attractiveness, the insulation property is also an important point. Both aluminum (Al) and low density polyethylene (LDPE) are practically recycled materials. Shopping bags and hoses are being recycled to be reused as the LDPE filling material between the two outer layers of aluminum sheets. Therefore, Al-LDPE-Al hybrid sandwich panels are environmentally friendly construction materials.

As the locations of applications vary, the panels have to withstand different climate conditions. The temperature may increase above 60°C under the sun and decrease -20°C in the winter time. The environmental friendliness through almost 100% recycled materials has on the hand a major drawback. The material quality is not constant and all these factors create a challenge to ensure the quality of the end product. The most of the problems and customer complaints were caused by the insufficient adhesion between polymer and metal layers. This study aims to provide a reliable method and a benchmark to ensure long-term adhesion quality of Al-LDPE-Al sandwich panels.

## Experimental Procedure

### Production of Sandwich Panels

Aluminum sheets of 5mm thickness, which are wound on rollers, are pre-treated for the panel production. The steps of pre-treatment on both surfaces of the aluminum sheet are oil removal, washing, acidic activation, washing, deionization, chromate and drying. Afterwards, upper surface is colored with polymer based dyes and the inner surface receives a back-coat for protection. The pre-treated sheets must enter the panel production within two days, otherwise the activated surface of aluminum for a better adhesion with polyethylene does not perform well.

The production steps of the sandwich panel are depicted in figure 1. The recycled LDPE first goes to the feeding area. The required weight of material is mixed and heated to 170°C in a mixer. The main extruder heats the polyethylene up to 200°C through six heating regions and pumps it into the mold to feed the material as a filling sheet form between the two aluminum sheets. The auxiliary extruder heats the adhesive up to 225°C to activate the anhydrite groups and pumps it through the mold, above and below the polyethylene filling. Two cylinders adjust the constant thickness of 4mm for the whole sandwich material package. Four cooling cylinders contact the panel only from the lower surface in order not to have a negative effect on the surface color. The cooling zone of 70°C (two sections as shown in the figure) has both resistance heating and air cooling to keep the temperature constant. After this section, an edge cutting mechanism cuts the rest material of filling polyethylene which makes a barrel shape out of the edges. The removed extra polyethylene again goes into the feeder. The cooling zone of 40°C with two sections works with air ventilation. After visual quality check, the protection foil is applied onto the outer surface of panel. The determined length of the panel, which is mostly 6m, is cut with a knife and pneumatic arms stack the panels.

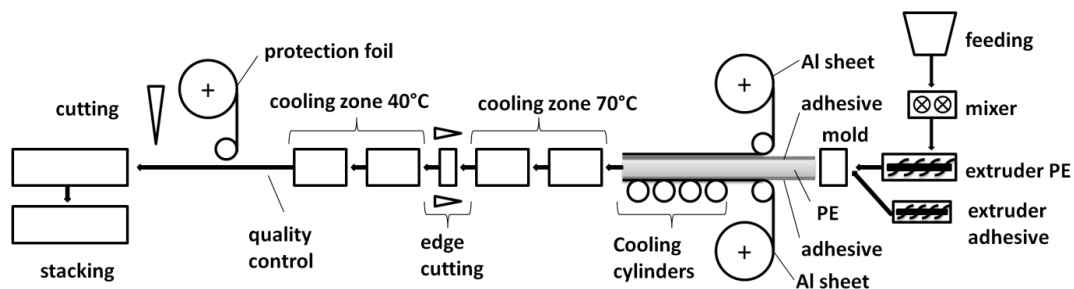


FIGURE 1. SCHEMATIC OF THE Al-LDPE-Al HYBRID SANDWICH PANEL PRODUCTION

### Testing of Adhesion

The adhesion between the aluminum layers and the polyethylene filling is tested according to DIN 53278. A standard tensile testing machine Z050 of the company Zwick GmbH with a special holding device for the peeling test is used. The schematic of the machine is shown in figure 2. The samples have the dimensions of 4mm thickness, 25mm width and 250mm length. The test machine has the preload of 2N and a testing speed of 150mm/min.

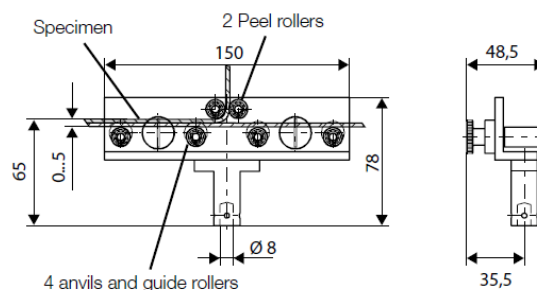


FIGURE 2. SCHEMATIC OF THE PEELING TEST DEVICE (COURTESY OF Zwick GmbH)

Taking couple of samples for the peeling test may give an idea about the overall adhesion between aluminum and polyethylene layers. However, as mentioned earlier above, the recycled polyethylene may yield inhomogeneous structure which has to be captured. The mechanical parts may also have improper adjustments or eccentricities

which are impossible to detect via visual investigations. Therefore, it is necessary to take samples which cover and scan a certain whole area of the panel. The longest circumference of the machine elements shown in figure 1 is 1.5m. The length of 2m is sufficient to observe the possible periodical footprints of an eccentric or unadjusted machine element. The standard width of the panel is 1m, so the peeling samples spread on 2m<sup>2</sup> surface in four lines (80 samples in each line) as shown in figure 3 because the length of the samples is 250mm. Immediately after the horizontal samples one line of 48 vertical samples are positioned to see the horizontal course of the adhesion values.

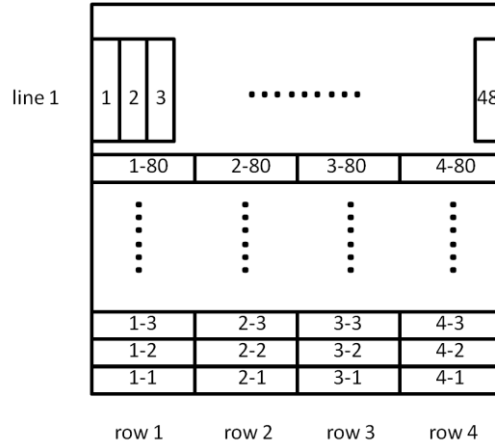


FIGURE 3. LOCATION OF PEELING SAMPLES ON THE PANEL

**Theoretical Approach**

Polyethylene is a recyclable and cost-efficient polymer. Its low viscosity is advantageous for the production point of view because the mixer and extruder devices have smaller dimensions than for other polymers and consume less power. However, the heat expansion coefficient of polyethylene is the highest among industrial polymers, which makes it a challenge to produce sandwich materials with polyethylene filling. In this case of sandwich panel, polyethylene yields nine times higher heat expansion coefficient than aluminum. Thus, the amount of adhesion strength must be calculated for this kind sandwich panel which is used as outer cover of buildings. Figure 4 shows the schematic of the sandwich panel and its relevant dimensions for the calculations. Table 1 gives the engineering constants and values for the panel.

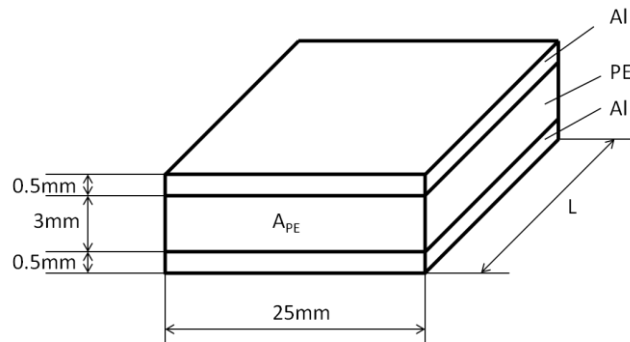


FIGURE 4. SCHEMATIC AND DIMENSIONS OF SANDWICH PANEL FOR CALCULATIONS

TABLE 1. ENGINEERING CONSTANTS AND VALUES FOR THE SANDWICH PANEL

EAl (GPa)	EPE (MPa)	APE (mm <sup>2</sup> )	αAl (μm/m.K)	αPE (μm/m.K)	ΔαAl-PE (μm/m.K)
70	450	75	23	200	177

Equation 1 formulates the linear expansion or shrinkage of a material caused by a change in temperature. The sandwich panels have to withstand the extreme temperatures of -15°C and 70°C in the climate of application areas.

$$\Delta L = L * \alpha * \Delta T \tag{1}$$

By entering the values of 85°C (which is same for Kelvin) for ΔT, 177μm/m.K for Δα, and L is any value in the unit of meters, ΔL can be found as 15.045\*L mm.

Equation 2 gives the strain value and equation 3 gives the relationship between stress and strain.

$$\epsilon = \Delta L/L \tag{2}$$

$$\sigma = E * \epsilon \tag{3}$$

Considering the unit of L as meter, the strain value is calculated  $15.045 \cdot 10^{-3}$  by using equation 2.

The stress caused by the above calculated strain is calculated with equation 3. The modulus of elasticity for polyethylene is 450MPa as given in table 1, which is multiplied with the strain value of  $15.045 \cdot 10^{-3}$ . The stress on the cross sectional area APE is calculated as 6.77MPa (N/mm<sup>2</sup>).

Another equation of stress  $\sigma$  is the ration of force to the cross sectional area which is given in the equation 4.

$$\sigma = F/A \tag{4}$$

So, the total force between the two layers aluminum and the polyethylene filling can be calculated by multiplying the stress 6.77MPa and the cross sectional area of 75mm<sup>2</sup> which is 507.75N. There are two layers of contact between aluminum and polyethylene, so each layer has to withstand about 254N (figure 5).

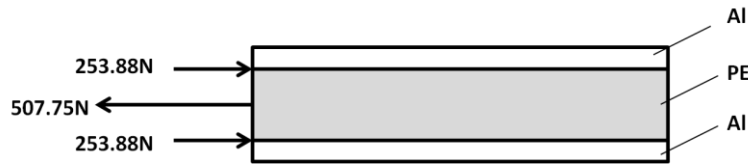


FIGURE 5. EQUILIBRIUM OF THERMAL EXPANSION FORCES

### Results and Discussion

The calculated value of 254N is based on the thermal shear stress between aluminum and polyethylene layers in case of an extreme temperature difference of 85°C. In reality, the panels go through two cycles of temperature change. One is the daily change of about 15°C, the other is the seasonal change of about 30°C. The assumption is that if the adhesion is enough for one time extreme temperature change, it should be enough for the cycles of much smaller temperature which changes over couple of years.

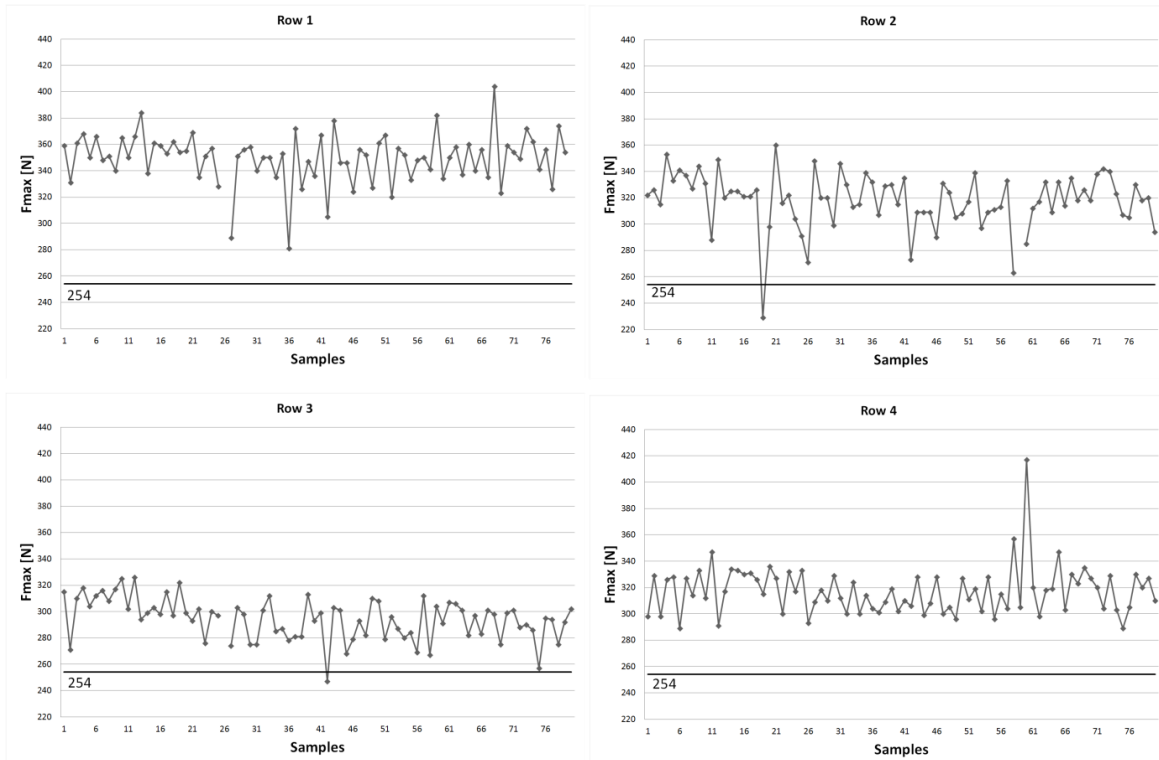


FIGURE 6. PEELING TEST RESULTS OF ROW 1-4

Figure 6 depicts the peeling test results of row 1 to 4. There are some missing points on the diagrams which were due to failures during measurement. Every row has 80 measurements which show the tendency of adhesion between aluminum and polyethylene. Each of rows 3 and 5 has only one point which is less than the set limit value of 254N. A distinctive periodical behavior of the curves would indicate a machine failure, where the period of the curve would give the circumference of the machine element. This would be helpful to identify a machine failure or an eccentricity. The results of row 1-4 do not show a significant periodical curve, which means that the machine settings do not have problems. There is still a deviation on the curves which is caused by the inhomogeneous recycled polyethylene and the mechanical vibrations during production.

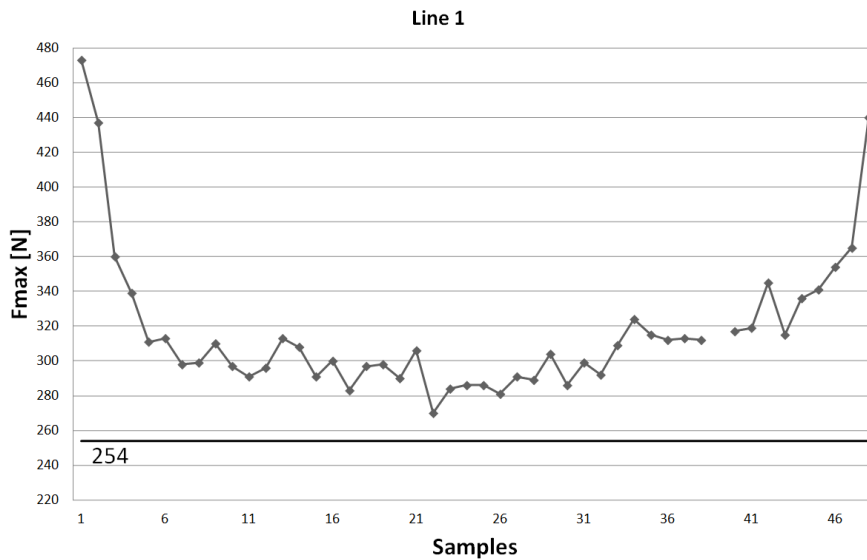


FIGURE 7. PEELING TEST RESULTS OF LINE 1

Figure 7 shows the horizontal course of the adhesion between the aluminum and polyethylene layers. The U-shaped curve is advantageous to keep the edges tighter for a possible mechanical stress during transportation or storage. There are four nozzles to adjust the flow of adhesive along the width. The machine elements work in the flow direction of the panel so it is very unlikely to see any periodical footprints on this curve. As the graphs of row 1-4, there is the effect of material and vibration.

The previous minimum limit of peeling test results was 100N which caused around 5% customer claims about insufficient adhesion. The new value of 254N was observed for six months and absolutely no claims came within this period of time about the insufficient adhesion. The observations will continue and the 254N minimum value seems to ensure a quality time of five years for adhesion of aluminum polyethylene sandwich panels. Scanning of the panel surface with 368 samples as shown in figure 3 will be applied whenever a new sort of recycled polyethylene is bought. The graphs in figures 6 and 7 show that the polyethylene quality is reliable that no significant variations in adhesion occur.

## Conclusion

The adhesion problem is analyzed within the scope of this study. The theoretical shear stress due to the extreme temperature change of 85°C is calculated. According to this thermal shear stress, an adhesion value of 254N between the aluminum and polyethylene layers is necessary. A surface of more than 2m<sup>2</sup> is scanned through peeling test. An observation period of six months has shown that this limit value is sufficient for the adhesion quality of aluminum polyethylene sandwich panels. The scanning of a whole surface gave additional information that the machine elements work properly and the recycled material quality is reliable.

## ACKNOWLEDGEMENTS

The author would like to thank his colleague Semih Ögrü for the friendly support during the execution of the trials.

**REFERENCES**

- [1] Khodabakhshi, F.; Haghshenas, M.; Sahraeinejad, S.; Chen, J.; Shalchi, B.; Li, J.; Gerlich, A.P. *Materials Characterization* 2014, 98, 73-82.
- [2] Paul, H.; Luke, M.; Hennig, F. *Composites: Part B* 2015, 73, 158-165.
- [3] Grujicic, M.; Sellappan, V.; Omar, M.A.; Seyr, N.; Obieglo, A.; Erdmann, M.; Holzleitner, J. *Journal of Materials Processing Technology* 2008, 197, 363-373.
- [4] Pesetskii, S.S.; Jurkowski, B.; Kuzavkov, A.I. *International Journal of Adhesion & Adhesives* 1998, 18, 351-358.
- [5] Jung, C.-H.; Cho, H.-W.; Hwang, I.-T.; Choi, J.-H.; Nho, Y.-C.; Shin, J.-S.; Chang, K.-H. *Radiation Physics and Chemistry* 2012, 81, 919-922.